11th Canadian Masonry Symposium, Toronto, Ontario, May 31- June 3, 2009

INFLUENCE OF SECOND ORDER EFFECTS ON SLENDER, UNREINFORCED MASONRY WALLS

Jennifer R. Bean Popehn[1], Arturo E. Schultz[2] and Jennifer E. Tanner[3]
[1] Assoc. Engineer, OPUS Architects & Engineers, Minnetonka, MN 55343, USA, jennifer.popehn@opus-ae.com
[2] Professor, Dept. of Civil Engineering, Univ. of Minnesota, Minneapolis, MN 55455, USA, schul088@umn.edu
[3] Asst. Prof., Dept. of Civil & Architectural Engineering, Univ. of Wyoming, Laramie, WY 82071, USA
tannerj@uwyo.edu

ABSTRACT
The buckling strength and deformation capacity of an unreinforced masonry wall (URM) can be significantly affected by both initial imperfections and axial load eccentricity. To account for this decrease in strength, the 2008 TMS-402 (i.e., United States (US) masonry design provisions) Strength Design chapter includes a new provision for including second order effects through a moment magnifier. However, this method of treatment has limitations: initial imperfections are essentially not considered when the eccentricity is larger than 10% of the wall thickness. Additionally, when designing using Allowable Stress Design (ASD), the second order bending effects arising from axial load are ignored. To determine the accuracy of the ASD and SD provisions, the calculated moment magnifiers were compared to experimental data from seven slender URM wall tests conducted at the University of Minnesota. In the experimental study, three of the walls were constructed of cored clay brick, while the remaining four were fabricated using hollow concrete block. The simply-supported masonry wall tests began with a pre-selected axial load which was applied to the walls in force control using two vertical load actuators and held constant throughout the tests. After the axial load was applied to the walls, lateral load was applied with a whiffletree system operated in displacement control. The lateral displacement was increased until all lateral load capacity had diminished.

KEYWORDS: slenderness, imperfection, second order, axial load eccentricity, unreinforced masonry, buckling strength

NOTATION
A_n = net cross-section area
C_m = factor relating to the actual moment diagram to an equivalent uniform moment diagram
E_m = modulus of elasticity of masonry
I_n = moment of inertia of cross-section about weak axis
M_a = first order moment due to axial load eccentricity (i.e., Pe_a)
M_w = first order moment from out-of-plane lateral loads (i.e., $wh^2/8$)
M_Δ = second order moment (i.e., $P\Delta$)
P = axial load

P_{Euler} = Euler's buckling load
P_u = factored axial load
e_a = axial load eccentricity
f'_m = specified compressive masonry strength
h = effective height of the wall
r = radius of gyration
w = uniformly distributed lateral load
Δ = maximum value of total deflection due to first and second order moments
δ = moment magnification
δ_{exp} = moment magnification based on experimental data (i.e., $(M_w + M_a + M_\Delta)/(M_w + M_a)$)
δ_{MSJC} = moment magnification based on 2008 TMS-402 design provisions
ϕ_k = stiffness reduction factor

INTRODUCTION

Unreinforced masonry walls (URM) are sensitive to both initial imperfections and axial load eccentricity, particularly when the walls are slender. An initial deflection of the wall can impair the buckling behavior of URM members by not only reducing the buckling capacity, but also by curtailing the deformation capacity. It has been noted that when a small negative initial imperfection (e.g. initial deflection) is present (i.e., on the order of 10% wall thickness), the capacity of the wall can be reduced to 40-55% of the critical load [1, 2]. For larger initial deflections (i.e., 40% wall thickness), the capacity of the wall could be diminished to 15-20% of the buckling load.

The 2008 TMS-402 (i.e., United States (US) Masonry Design Provisions) currently addresses the influence of eccentricity of a compressive axial load through the calculation of the critical buckling strength [3]. However, this method of treatment has limitations: initial imperfections are essentially not considered when the eccentricity is larger than 10% of the wall thickness. Additionally, when designing using Allowable Stress Design (ASD), the second order bending effects arising from axial load are ignored. The rationale for avoiding a moment magnifier term was that for practical rages of h/r, the errors induced by ignoring the moment magnifier are relatively small (i.e., less than 15%). Additionally, where moment magnification is more critical (e.g., slender walls with larger h/r values), the allowable axial load on the member is limited by code (i.e., $¼P_e$), and the overall safety factor is sufficiently large to allow the simplification in design procedure [3].

When using strength design (SD) of masonry, a new provision was added to the 2008 TMS-402 for including second order effects through a moment magnifier. The moment magnifier is based on the ACI 318 moment magnifier formula and has been modified to include the masonry material properties (Equation 1).

$$\delta = \frac{1}{1 - \dfrac{P_u}{A_n f'_m \left(\dfrac{70r}{h}\right)^2}} \tag{1}$$

This equation was derived from the general moment magnifier formula, Equation 2, where the Euler buckling load is given by Equation 3. To obtain Equation 1 from Equation 2, it was assumed that the masonry modulus of elasticity, E_m, was equal to $700f'_m$, which is the assumed value for clay brick masonry in Chapter 1 of the TMS-402 design provisions [3]. The stiffness coefficient, ϕ_k, was derived to be equivalent to 0.71, which closely approximates the 0.75 that is assumed for reinforced concrete design [3]. It was also assumed that the walls were simply supported and that C_m was equal to unity.

$$\delta = \frac{C_m}{1 - \frac{P_u}{\phi_k P_{Euler}}} \tag{2}$$

$$P_{Euler} = \frac{\pi^2 E_m I_n}{h^2} \tag{3}$$

EXPERIMENTAL STUDY

To determine the accuracy of the ASD and SD provisions, the calculated moment magnifiers capacities were compared to magnifiers calculated using experimental data from seven slender unreinforced masonry wall tests conducted at the University of Minnesota. In the experimental study, three of the walls were constructed of cored clay brick, while the remaining four were fabricated using hollow concrete block. All walls were laid in running bond using Type S Portland cement-lime mortar. The brick walls had full mortar beds, while the block walls had face-shell bedded joints. A complete list of material properties for the experimental specimens is given in Table 1.

Table 1: Material Properties

	Concrete Block	Clay Brick
A_n, cm^2(in^2)	572 (88.7)	628 (97.4)
A_g, cm^2(in^2)	745 (115)	723 (112)
E_m, MPa (psi)	12,200 (1,770,000)	13,200 (1,920,000)
P_{Euler}, kN (kips)	518 (116)	598 (134)
b, mm (in.)	803 (31.6)	803 (31.6)
f'_m, MPa (psi)	18.4 (2670)	32.5 (4720)
h_e, m (in.)	3.48 (137)	3.26 (128)
t, mm (in.)	92.7 (3.65)	89.9 (3.54)

The experimental program was designed around the test setup shown in Figure 1, with some modifications made after testing the first three walls, which is discussed in a later section. The simply-supported masonry wall tests began with a pre-selected axial load which was applied to the walls in force control using two vertical load actuators and held constant throughout the tests. Brick walls B1-25, B2-50, and B3-70 supported axial loads of 111 kN (25 kips), 222 kN (50 kips), and 311 kN (70 kips), respectively, as noted in the latter number in the wall designation. These axial loads represent 19%, 37%, and 52% of the Euler buckling load (Eqn. 3) for walls B1-

25, B2-50, and B3-70, respectively. Concrete block walls C1-15, C2-30, C3-50 and C4-75 sustained axial loads of 66.7 kN (15 kips), 133 kN (30 kips), 222 kN (50 kips), and 334 kN (75 kips), which represent 13%, 26%, 43%, and 64% of the Euler buckling load, respectively. In calculating the Euler loads for these walls, no allowance was made for the influences of the lateral loads, cracking, or any accidental eccentricity of axial load, and the TMS-402 definition for masonry modulus was used [3].

After the axial load was applied to the walls, lateral load was applied with a whiffletree system, which was comprised of threaded steel rods and spreader beams (Fig. 1). It loaded the masonry panels along two vertical lines and at four elevations along the wall height, which produced a lateral moment distribution that closely simulated the moment diagram for uniform lateral pressure [4]. The actuator was operated in displacement control; and lateral displacement was constantly increased until the wall specimens lost all capacity to resist lateral loading. Thus, during the tests, the specimens also resisted second-order (P-Δ) moments generated by the applied axial force multiplied by the lateral deflection of the wall. The loading and the specimen response to loading were measured using internal load cells in the actuators, horizontal load cells on the whiffletree, and displacement transducers at various locations.

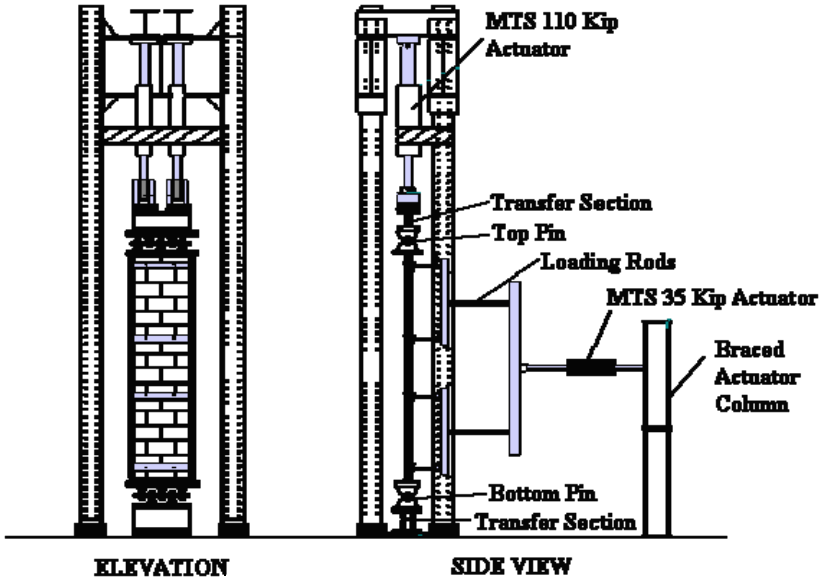

Figure 1: Load frame for Unreinforced Masonry Wall test

After testing the first three wall specimens, a problem regarding the testing assembly was discovered: the bearings that were used to simulate pin supports at the top and bottom of the specimens did not behave as frictionless pins in the presence of vertical load, and moment restraint was generated at the ends of the wall specimens during these tests. To alleviate the flexural restraint at the pins, spherical roller bearings were used in place of the original pins, and no evidence of moment restraint was noted for the remaining walls tests (i.e., C1-15, C2-30, C3-50, and C4-75). However, the first three wall specimens (Walls B1-25, B2-50, and B3-70) were not tested in the desired simply-supported configuration, but rather one with unknown flexural restraints at the ends. In order to use the data from tests B1-25, B2-50, and B3-70, a careful evaluation of the distribution of lateral displacement was used to locate of the points of inflection

at different stages of the tests. The resulting lateral displacement profiles were used to generate curvature profiles, from which the points of inflection were identified [5].

The locations of the points of inflection were used to define the effective height h_e of the specimens. At the time of peak lateral loading, the effective height factor, $k = h_e/h$, was found to be equal to 0.74 for both specimens B2-50 and B3-70 and the same effective height factor was assumed for specimen B1-25 (i.e., $k = 0.74$) since this procedure could not be used for Wall B1-25 due to insufficient sensor data. Thus, Walls B1-25, B2-50, and B3-70 were less slender than planned (i.e., $kh_e/r = 126$). Evaluation of lateral displacement profiles for walls tested using the modified setup (i.e., C1-15, C2-30, C3-50, and C4-75) indicated that the effective heights were equal to the actual height (i.e., $k = 1$ and $h_e/r = 115$).

COMPARISONS OF CALCULATED TO EXPERIMENTAL MOMENT MAGNIFIERS

The experimental moment magnifier (Equation 4) of the test specimens can be determined from the moments due to applied lateral load, axial load eccentricity, and second order effects (Figure 2). The moment due to lateral load, M_w, was determined using the whiffletree load cell data assuming a uniformly distributed load. The moment due to axial load eccentricity, M_a, and the second order moment, M_Δ, were calculated using the output from the vertical actuator and inferred vertical load eccentricities [5] and recorded mid-height lateral displacement at peak lateral load, respectively.

$$\delta_{\text{exp}} = \frac{M_w + M_a + M_\Delta}{M_w + M_a} \tag{4}$$

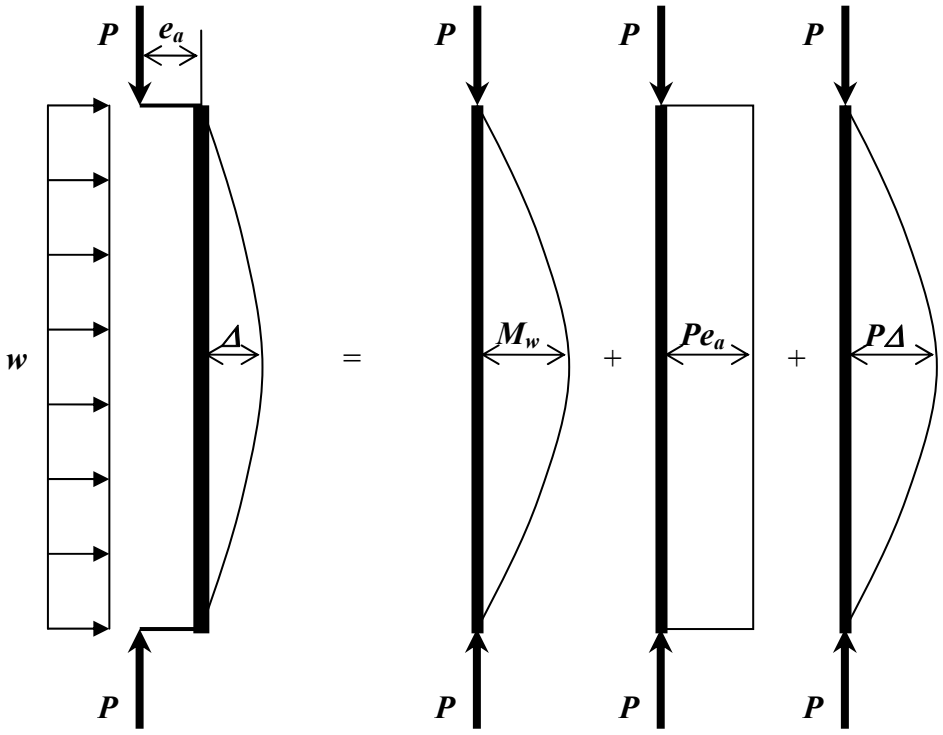

Figure 2: Idealized Wall Response

During the experimental tests, the masonry wall specimens exhibited behavior during the axial loading stage of the tests that was consistent with initial imperfections in the 'trueness' or 'straightness' of the members. These imperfections were the result of construction variations (e.g., different unit sizes and misalignment of units), as well unintentional misalignment of the test setup. The initial imperfections manifested themselves as lateral deflections that increased with increasing axial compression, and they were evaluated using measured member responses to axial loading because slender URM walls are sensitive to axial load eccentricity [5]. Small amounts of unintentional lateral loads were also applied as the walls attempted to deflect laterally due to the configuration of the lateral loading system. The inferred total axial eccentricity was 2.8 mm (0.11 in.), 4.6 mm (0.18 in.), and -0.76 mm (-0.03 in), for brick walls B1-25, B2-50, and B3-70, respectively. For the block walls C1-15, C2-30, C3-50, and C4-75, the inferred eccentricities were 2.8 mm (0.11 in.), 3.1 mm (0.12 in.), -2.3 mm (-0.09 in.), and 3.1 mm (0.12 in.), respectively.

Figure 3 shows the comparison between the calculation of the moment magnifier using the TMS-402 code formula (Equation 1) and the experimental moment magnifier determined using Equation 4. The brick walls demonstrated less variability (i.e., COV = 0.11) than the block walls (i.e., COV = 0.31). However, for the brick walls, the calculated moment magnifier using Equation 1 was generally smaller than the experimental value, which is undesirable. It is also noted that for the three wall tests that meet the TMS 402 buckling load requirement (i.e., $P < ¼ P_e$ as indicated by the horizontal axis), the average ratio is 0.95 and the standard deviation is 0.18. This finding is not surprising since the equations were developed with the assumption that the axial compression was significantly lower than the critical buckling load.

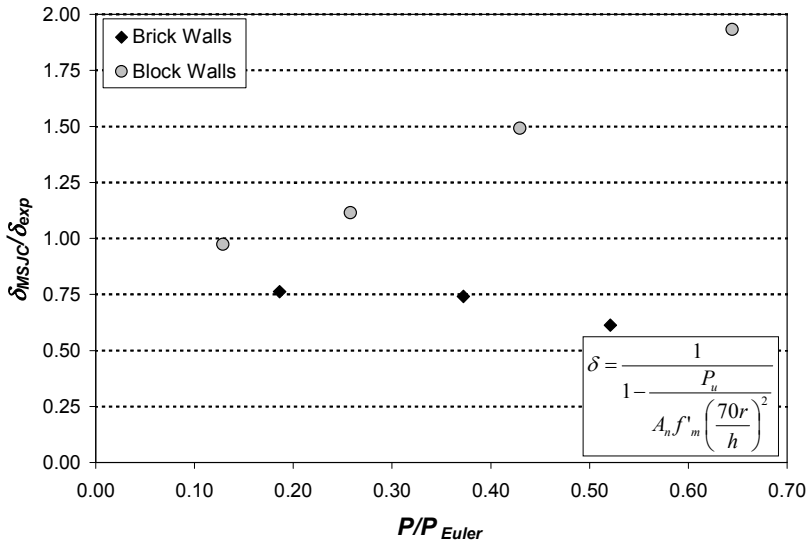

Figure 3: Comparison of Calculated MSJC-to-Experimental Moment Magnifier using Equation 1

Another comparison was made using the calculated general moment magnifier formula, Equation 2, where the Euler buckling load was determined with Equation 3. The value of C_m was equal to unity, since the experimental tests were simply supported, and the axial load used in the denominator was the axial load applied in the experimental tests. The stiffness reduction factor

was assumed to be 0.75, which is consistent with reinforced concrete. By using Equation 2, the measured modulus of elasticity of the wall is utilized, rather than the inherent assumption of E_m = 700f'_m in Equation 1.

When these calculated ratios were compared to the experimental ratios calculated using Equation 4 (Figure 4), better results were obtained for the brick walls: the average magnifier ratio was 1.01 with a standard deviation of 0.15. The block wall data exhibited little change when comparing it to Figure 3 because the term in the denominator of Equation 1 (e.g., $A_n f'_m (70r/h)^2$) gave buckling loads within 2% of that from Equation 2 (e.g., $\phi_k P_{Euler}$). For the brick walls, the term $A_n f'_m (70r/h)^2$ calculated using Equation 1 (Figure 3) was 62% higher than $\phi_k P_{Euler}$ used in the denominator of Equation 2 (Figure 4). This result is consistent with the assumed modulus of elasticity used in Equation 1 (i.e., E_m = 700f'_m) over-predicting the experimental modulus of elasticity by a factor greater than 2.

This result demonstrates that the inherent assumption of the modulus of elasticity in Equation 1 (i.e., 700f'_m for both concrete block and clay brick) is not appropriate for all wall types. The TMS-402 [3] design provisions approximate the clay and concrete masonry modulus of elasticity values as 700f'_m and 900f'_m, respectively. With that in mind, the measured moduli for the clay brick and concrete block experimental wall tests were 400f'_m and 660f'_m, respectively, which is significantly lower (i.e., 58% and 73%, respectively) than the TMS-402 values.

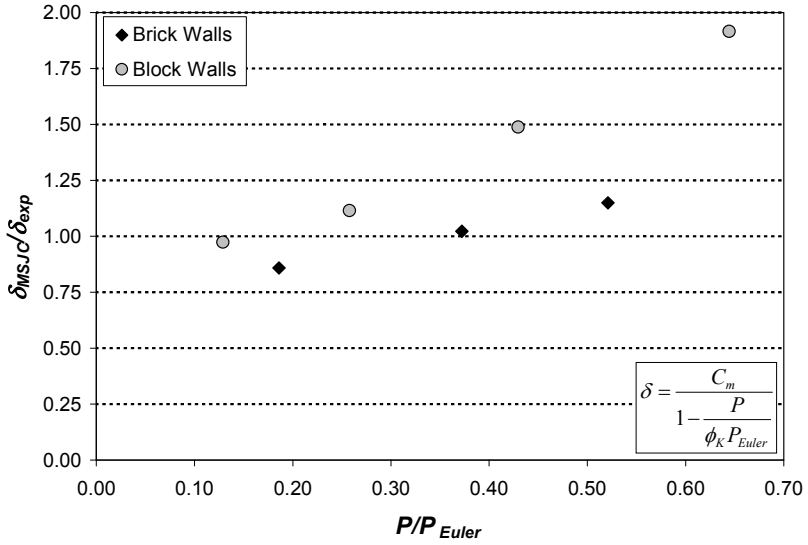

Figure 4: Comparison of Calculated MSJC-to-Experimental Moment Magnifier using Equation 2

Since the ratio in the denominator of Equation 1 and Equation 2 was seen to play a significant role in the accuracy of the moment magnifier, another approach was investigated. Rather than using a reduction factor, ϕ_k, for the Euler buckling load, P_{Euler}, the latter was calculated taking into account the axial load eccentricity (Equation 5) using the TMS-402 allowable stress design formula for eccentric buckling [3].

$$P_e = \frac{\pi^2 E_m I_n}{h^2}\left(1 - 0.577\frac{e_a}{r}\right)^3 \quad (5)$$

The inferred experimental eccentricities of the wall tests ranged in magnitude between -2% to +5% of the wall thickness. These eccentricities are within the assumed eccentricity of Equation 1 (i.e., 10% of the wall thickness). If the inferred eccentricity is used to determine the moment magnifier using Equation 5, the calculated-to-experimental magnifier ratios are closer to unity (Figure 5), even for axial load ratio greater than allowed by code (i.e., $P > ¼\ P_e$). The brick wall ratios averaged 0.86 with a standard deviation of 0.18, and the block walls had an average of 1.05 with a standard deviation of 0.09. These results give a coefficient of variation of 0.20 and 0.08 for the brick and block walls, respectively. It is also noted that the effects of cracking from lateral loading were neglected. If this effect was included, the magnitude of P_e would be decreased further and the magnifier would increase.

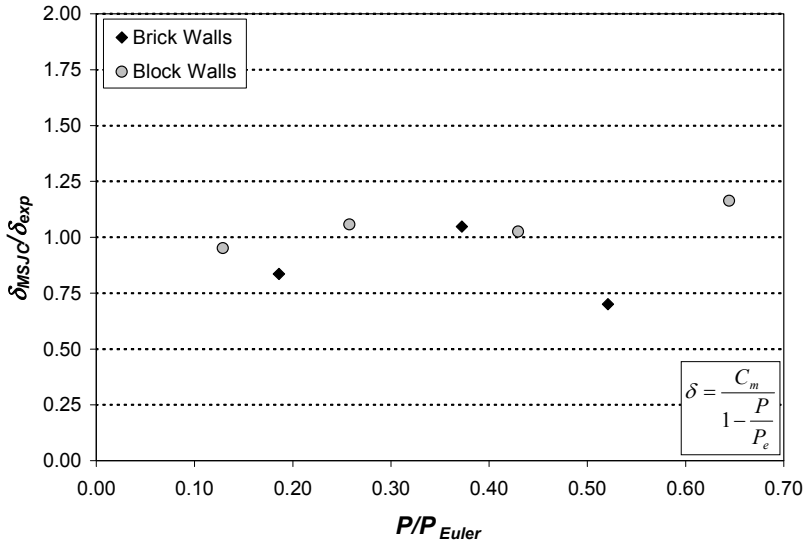

Figure 5: Comparison of Calculated MSJC-to-Experimental Moment Magnifier using Equation 5

CONCLUSIONS

The strength and deformation capacity of unreinforced masonry walls depend not only on the wall section properties, but also any initial imperfections and eccentricity of the axial load. Stocky URM walls are not as dependent on these variables, but they can have a significant influence on the strength of slender walls. The 2008 TMS-402 (i.e., US Masonry Design Provisions) addresses the compressive axial load eccentricity influence through the calculation of the critical buckling strength [3]. This method does have limitations, namely through assumptions in the magnitude of the modulus of elasticity and initial imperfections, as well as the strength reduction coefficient resulting from imperfections.

When using Strength Design (SD) of masonry, a new provision was added to the 2008 TMS-402 for including second order effects through a moment magnifier. The moment magnifier is based on the ACI 318 moment magnifier formula and has been modified to include the masonry material properties (Equation 1).

To determine the accuracy of this equation, the calculated moment magnifier was compared to magnifiers determined from an experimental study at the University of Minnesota. The study included tests of seven unreinforced masonry walls (3 clay brick and 4 concrete block walls) subject to axial compression and lateral loading.

Using the TMS-402 design equation to calculate the moment magnifier (Equation 1), comparisons were made to the magnifiers determined from the experimental tests, and the results showed coefficients of variation of 0.11 and 0.31 for the brick and block walls, respectively. Another comparison was made using the calculated general moment magnifier formula (Equation 2) with the Euler buckling load in the denominator, which did not have an inherent assumption on the magnitude of the modulus of elasticity. With this equation, the comparison of the calculated-to-experimental magnifier ratios showed better results for the brick walls and little change for the block wall ratios. This result demonstrated that the assumption of the modulus of elasticity magnitude in Equation 1 is not appropriate for all walls. A last comparison was made using Equation 5, where the critical buckling load was calculated using the magnitude of the axial load eccentricity. This method produced calculated-to-experimental magnifier ratios closer to unity, even for axial load ratios greater than allowed by code (i.e., $P > ¼\ P_e$). Additionally, the brick wall moment magnifier ratios averaged 0.86 with a standard deviation of 0.18, and the block walls had an average of 1.05 with a standard deviation of 0.09.

The results obtained demonstrate that the assumptions of the magnitude of the modulus of elasticity and axial load eccentricity have a strong influence on the magnitude of the calculated moment magnifier. Further study is needed in this area, and the influence of these parameters should also be investigated on the stability of reinforced and post-tensioned masonry walls.

REFERENCES

1. Lu, M., Schultz, A. E., and Stolarski, H. K. (2004). "Analysis of the Influence of Tensile Strength on the Stability of Eccentrically Compressed Slender Unreinforced Masonry Walls under Lateral Loads." *Journal of Structural Engineering*, American Society of Civil Engineers, 130(6): pp. 921-933.
2. Lu, M. (2003). "Stability of Unreinforced Masonry Members under Simultaneous Vertical and Out-of-Plane Lateral Loads," Ph.D. dissertation, University of Minnesota.
3. Masonry Standards Joint Committee. (2008). "Building Code Requirements for Masonry Structures." TMS 402/ACI 530/ASCE 5, USA.
4. Bean, J. R. (2003). "Experimental Verification of the Resistance of Masonry Walls under Transverse Loads," M.S. Thesis, University of Minnesota.
5. Bean Popehn, J. R., Schultz, A. E., Lu, M., Stolarski, H, K., and Ojard, N. J. (2008). **"**Influence of Transverse Loading on the Stability of Slender Unreinforced Masonry Walls", *Elsevier* Journal of Engineering Structures, Vol. 30, Issue 10, pp. 2830-2839